Kasetsart J. (Nat. Sci.) 47 : 302 - 309 (2013)

Computer Simulation and Experimental Investigations of Wall-Thickness Distribution in High Impact Polystyrene and Amorphous Polyethylene Terephthalate Thermoformed Parts

Teerapol Kittikanjanaruk and Somjate Patcharaphun*

ABSTRACT

The focus of this study was to determine the influence of molding parameters such as types of mold, sheet and mold temperatures on the wall-thickness distribution of thermoformed parts. The materials used were high impact polystyrene (HIPS) and amorphous polyethylene terephthalate (A-PET). All the thermoformed parts were molded only after the machine had attained a steady state with respect to the preset sheet temperature from 130 to 170 ^{o}C and mold temperature of 30, 60, and 80 ^{o}C, respectively. Several settings were tried and those leading to an overall satisfactory quality with regard to visual properties were finally chosen. Furthermore, the commercial simulation package (T-SIM) was also extensively verified against experiments performed with simple mold geometry as well as with a more complicated part. Both simulated and measured results suggested that in order to obtain a more uniform wall thickness throughout the entire area of a thermoformed part, it was necessary to use a plug mold as well as a suitable mold temperature. The numerical results were in good agreement with the experimental ones, which suggested that the simulation program can be used as a valuable tool for avoiding the time-consuming and burdensome trial-and-error process.

Keywords: thermoforming process, processing parameters, thickness distribution, computer simulation.

INTRODUCTION

Thermoforming is an important process in the packaging industry, especially for thermoplastic materials because of their low cost and good formability (Throne, 1986). Other applications include making large parts such as refrigerator door liners, bathtubs, signs and automotive interior trim. A sheet is first clamped in a frame and is heated to a desired temperature above its glass transition temperature (T_g), so that it becomes rubbery and soft. It is then placed over a mold and is stretched to take the contours either of the cavity or plug mold, as schematically illustrate in Figure 1. Thermoforming has advantages over its better known competitor processes such as injection and extrusion blow molding processes, because it uses simpler molds and a much lower forming pressure. Although the thermoforming process has been developed for over two decades, there are still several unresolved problems that confound the overall success of this technology. Among them, non-uniform wall thickness distribution is most prevalent, caused by inappropriate mold

Department of Materials Engineering, Faculty of Engineering, Kasetsart University, Bangkok 10900, Thailand.
* Corresponding author, e-mail: fengsjpc@ku.ac.th

Received date : 28/09/12 Accepted date : 03/01/13

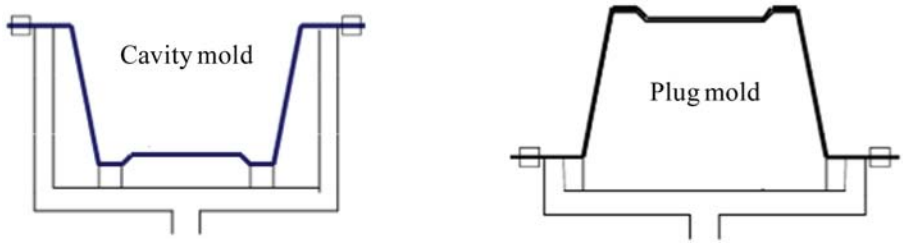

Figure 1 Two basic thermoforming molds.

design and processing conditions, since to achieve uniform wall thickness distribution, it is important to optimize the process before molding a part (Throne, 1986). For the purpose of cost reduction, the thermoplastic sheet needs to be employed as thinly as possible. Conventionally, the molders optimize the thickness of thermoformed parts by a time-consuming trial-and-error process. This approach involves the variation of processing conditions until an overall satisfactory quality with regard to mechanical and visual properties is reached.

Poller and Michaeli (1992) studied the effects of plug and film temperatures on wall thickness. They reported that plug and film temperatures are the major influencing parameters on wall thickness distribution when a plug-assist thermoforming method was used. However, Lai and Holt (1975) showed that a plastic film temperature in the range of 150 to 170 ^{o}C for polymethyl methacrylate (PMMA) and 110 to 130 ^{o}C for high impact polystyrene (HIPS) had no effect on the wall thickness distribution when the plastic sheets were formed into domes. On the other hand, the forming temperature was pointed out as a prominent parameter affecting the sagging and drawability of a plastic sheet (Rosenzweig *et al.*, 1979). Aroujalian *et al.* (1997) studied the influence of plug velocity and sheet and plug temperatures on the wall thickness distribution in plug-assist vacuum thermoformed containers using HIPS. The study showed that the wall location, plug temperature, plug velocity and their interactions influenced the wall thickness. However, the film temperature did not have a significant effect on the wall thickness and variation factor.

In recent years, thermoforming simulation software packages have been developed to predict the forming behavior and the wall thickness distribution of the final product, including T-FORMCAD (Polydynamics Inc.; Dundas, Ontario, Canada) and TFORM3 ® (Transvalor S.A.; Trondheim, Norway), which are commercially available. Various constitutive equations such as Mooney-Rivlin, Ogden and G'Sell (Dong and Lin, 2006) have been used with various simulation software packages to describe the extensional stress and strain behavior of a polymer. The advantages and disadvantages of these constitutive equations used to describe the extensional behavior of a polymer have been reported by Koziey (1997). In the current experimental work, the effects of sheet and mold temperatures on the wall thickness distribution of a thermoformed part using simple plug and cavity molds were investigated. The T-SIM simulation software (Accuform; Aachen, Germany) was also employed for the prediction of thickness distribution under different processing conditions. T-SIM utilizes a nonlinear time-dependent K-BKZ model which was proposed by Kaye (1962) and Bernstein *et al.* (1963). The model prediction was then compared with experimental results to gain a further basic understanding of the thermoforming process.

MATERIALS AND METHODS

The material used in this study were high-impact polystyrene (HIPS) and amorphous polyethylene terephthalate (A-PET), supplied in sheet form (thickness of 1 mm) by Wing Fung Packaging Co., Ltd., Thailand. The thermoformed part was carried out on a thermoforming machine (Model: SB-4060; BOSCO; Bangkok, Thailand). All the specimens were formed after the machine had attained a steady state with respect to the preset sheet and mold temperatures. The selection of the variation range for each material was based on the processing technique recommended by the material supplier. The effects of sheet and mold temperatures were varied on three levels, while other variables including vacuum pressure and cooling time were maintained at a constant level throughout this study. Table 1 summarizes the materials information and the various parameter settings. For the investigation of the thickness distribution, the thermoformed parts were cut along the axial direction. The sections were then mounted on a stage, after polishing with the help of a metallurgical technique. The thickness fraction of formed specimens was assessed by optical microscopy (Model PMG3; Olympus; New York, NY, USA) and computer-aided image analysis (Image-Pro Plus 5.1; Media Cybernetics, Inc., Rockville, MD, USA). The measurements were taken at every 2 mm from the edge, which corresponded to the measured distance ratio between the length of measurement and the total length of the specimen (78 mm).

The commercial software package, T-SIM, was used to predict the wall-thickness of the thermoformed part. First, the mold geometry was created by a computer-aided design program as schematically shown in Figure 2a. The sheet model (Figure 2b) was meshed by creating triangular elements on the surfaces (97,461 elements) and was then simulated using the finite element method, which is based on the K-BKZ non-linear and time-dependent viscoelastic material (Aleksey, 1995). The time-integral constitutive equation of the K-BKZ model is given by Equation 1:

$$\hat{\sigma}(t) = \int_{-\infty}^{t} \mu(t-\acute{t}) \cdot h(I_1, I_2) \cdot \hat{B}(t, \acute{t})\, d\acute{t} \qquad (1)$$

where $\hat{\sigma}(t)$ is the stress tensor, $\mu(t-\acute{t})$ is a time-memory function, $h(I_1,I_2)$ is a damping function of the two strain invariants I_1,I_2 and $\hat{B}(t)$ is the Finger strain tensor. Temperature effects are included via an Arrhenius temperature dependency of the material parameters. The time-memory function was calculated using Equation 2:

$$\mu(t-\acute{t}) = \sum_{i=1}^{N} \left\{ \frac{a_i}{\tau_i} \cdot e^{\frac{(t-\acute{t})}{a_i}} \right\} \qquad (2)$$

where a_i is the relaxation modulus, τ_i are the relaxation times and N is the number of the pair module per time.

The damping function $h(I_1,I_2)$ can be defined by one of Equations 3, 4 or 5:

$$h(I_1, I_2) = \frac{1}{1+\alpha\sqrt{(I_1-3)\cdot(I_2-3)}} \qquad (3)$$

Table 1 Materials information and variation of parameter settings.

Material	Tg (°C)	Density ($g.cm^{-3}$)	Thermal Conductivity ($W.m.^{-1}.°C^{-1}$)
HIPS 350E	95	1.04	0.12–0.18
A-PET	75	1.37	0.15–0.24
Parameter		Cavity mold	Plug mold
Sheet temperature (°C)		130/150/170	130/150/170
Mold temperature (°C)		30/60/80	30/60/80
Cooling time (sec)		15	15

Tg = Glass transition temperature, HIPS = High-impact polystyrene, A-PET = Amorphous polyethylene terephthalate.

$$h(I_1, I_2) = \frac{1}{\exp(\beta\sqrt{\alpha I_1 + (1-\alpha)\cdot(I_2 - 3)}} \quad (4)$$

$$h(I_1, I_2) = \frac{\propto}{(\alpha - 3) + \beta I_1 + (1-\beta)\cdot I_2} \quad (5)$$

where α and β are adjustable parameters and I_1,I_2 are the first and the second invariants of the Finger strain tensor given by Equation 6:

$$\hat{B}(t, \acute{t}) = \begin{bmatrix} \lambda^2(t, \acute{t}) & 0 & 0 \\ 0 & \lambda^{2m}(t, \acute{t}) & 0 \\ 0 & 0 & \lambda^{-2(1+m)}(t, \acute{t}) \end{bmatrix} \quad (6)$$

where λ is the extension ratio.

RESULTS AND DISCUSSION

Figure 3a shows the comparison of the wall-thickness distribution of the specimens formed by the cavity and plug molds. In the case of the cavity mold, the wall-thickness particularly decreased with an increase in the distance from the edge to the bottom of the part. The thinnest location of 0.10 mm occurred at the corner which represents only 10% of the original thickness. As can be clearly seen in Figure 3b, showing the plug- and cavity-formed units side by side for comparison, the deformation location and degree are quite obvious. The bottom of the cavity-molded

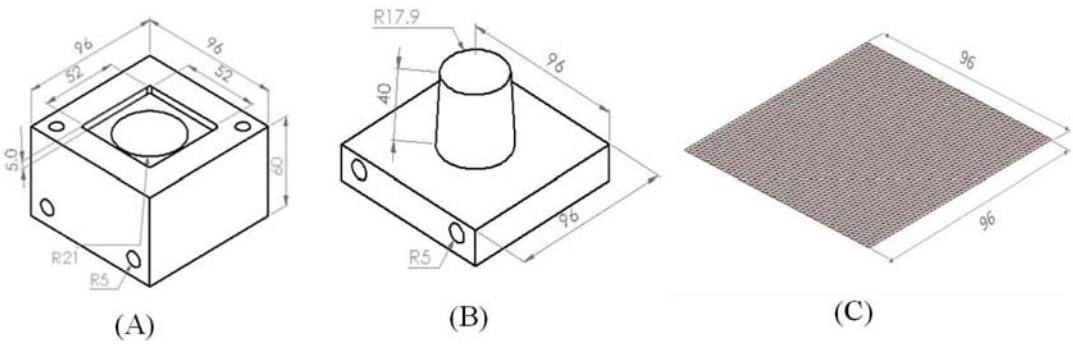

Figure 2 Geometry of: (A) Cavity mold; (B) Plug mold; (C) Mesh sheet used for the simulation. (All figures are distances in millimeters, R = radius.)

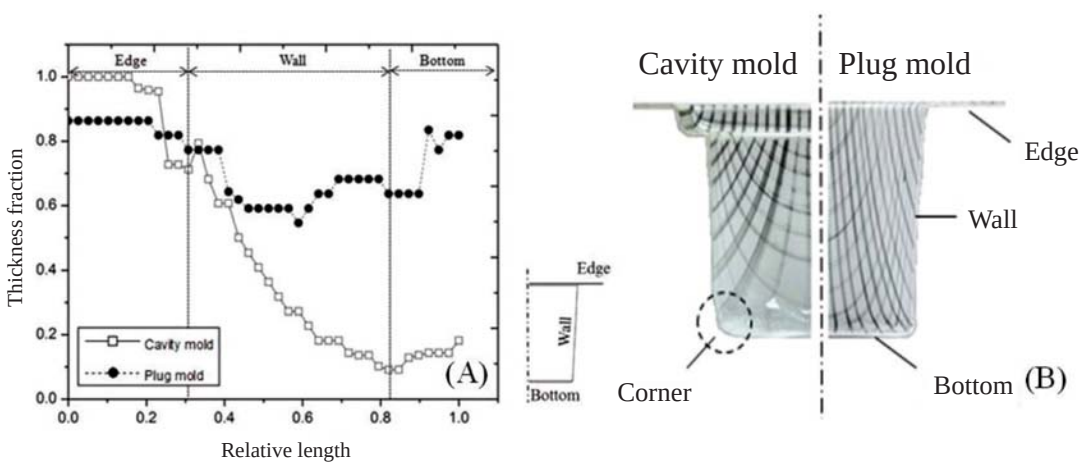

Figure 3 (A) Comparison of thickness distribution for thermoformed parts using cavity and plug molds; (B) Cavity formed part (left) and plug formed part (right).

part (especially around the corner) was very thin due to extreme stretching, while the bottom of the plug-molded part was nearly unchanged from the edge. The thinnest location of 0.6 mm occurred at the wall and represents 60% of the original thickness.

The effect of sheet temperature is depicted in Figures 4a and 4b. In this case, only the sheet temperature was varied and the mold temperature was kept unchanged. It can be seen that an increasing sheet temperature does not lead to substantial changes in the thickness distribution especially for the cavity-formed part. In both the cavity- and plug-formed parts, acceptable differences with regard to the thickness fraction values were noted between the measured positions. Probably, this can be attributed to the very high cooling rate at the mold wall which had a great effect on the viscosity of sheet. Differences can be only observed at the area of the edge thickness for the plug-formed part where the thicker edge is found due to increasing sheet temperature. Figures 5a and 5b show the effect of mold temperature on the thickness fraction of the cavity- and plug-

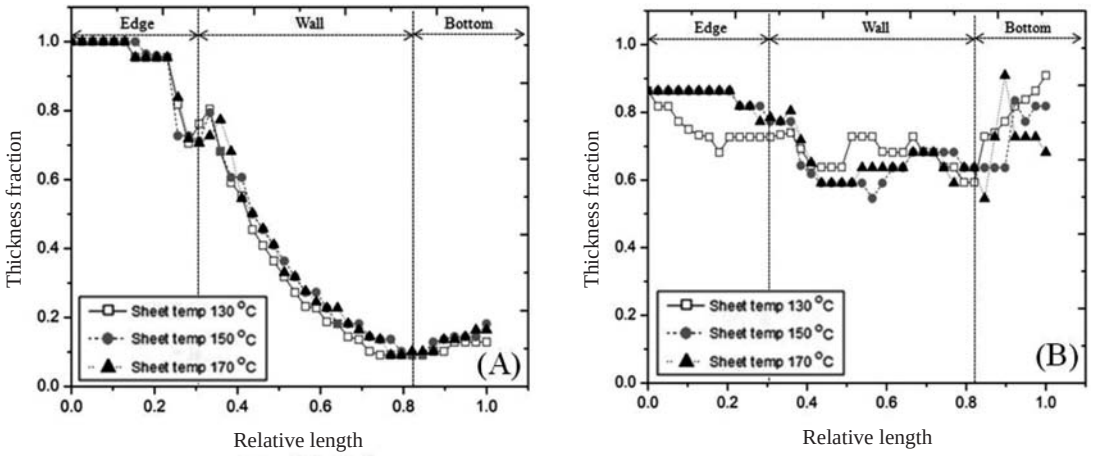

Figure 4 Influence of sheet temperature on thickness distribution: (A) Cavity-formed part; (B) Plug-formed part.

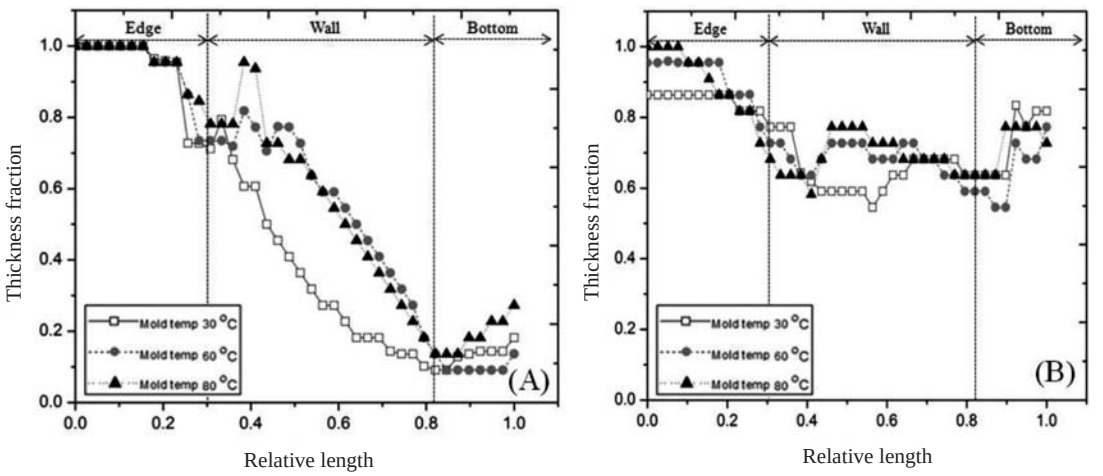

Figure 5 Influence of mold temperature on thickness distribution: (A) Cavity-formed part; (B) Plug-formed part.

formed parts. It should be noted that an increase in the mold temperature induces an increase in the thickness of the wall, as is clearly seen in the cavity-formed part. These results also indicated that an increase in mold temperature leads to an increasing edge thickness of the plug-formed part.

Figures 6a and 6b show the experimental and computer simulation results obtained from the cavity- and plug- formed specimens. It can be seen from Figure 6a that the predicted values of the thickness fraction throughout the entire length of the cavity-formed part agree very well with the measured data. However, it should be noted that the values for the thickness fraction of the plug-formed part are still different in that the predicted values were slightly lower than the measured values. This was probably due to the assumption of a steady state, in that the density, thermal conductivity and heat capacity of the polymer sheet, including the heat transfer and the friction coefficient, were assumed to be constant during the simulation, whereas in the real situation, these conditions are very difficult to achieve.

For a case study in complex geometry (a food tray), the thermoformed mold and product details are shown in Figures 7a and 7b. The A-PET film (thickness of 0.5 mm) was used and the sheet and mold temperatures were set at 150 and 30 ^{o}C, respectively. The simulation result of the wall thickness is given in terms of the thickness fraction, as shown in Figure 8. At the end of the forming state (see Figure 8a), the dark area designates the area where the thickness remains unchanged (near the edge), while the light area indicates the area where the sheet deforms to a desired shape. A comparison between the measured and simulated results for the food tray is shown in the graph in Figure 8b. It can be seen that the predicted values of the thickness fraction were also in accordance with the measured ones, although there was still a slight discrepancy.

CONCLUSION

The influences of processing parameters on the thickness distribution of thermoformed products were determined. The accuracy of the commercial simulation package (T-SIM) was verified by comparing its predictions with the corresponding experimental measurements. A good agreement between the simulated and experimental results indicated that the simulation program can be employed during the design

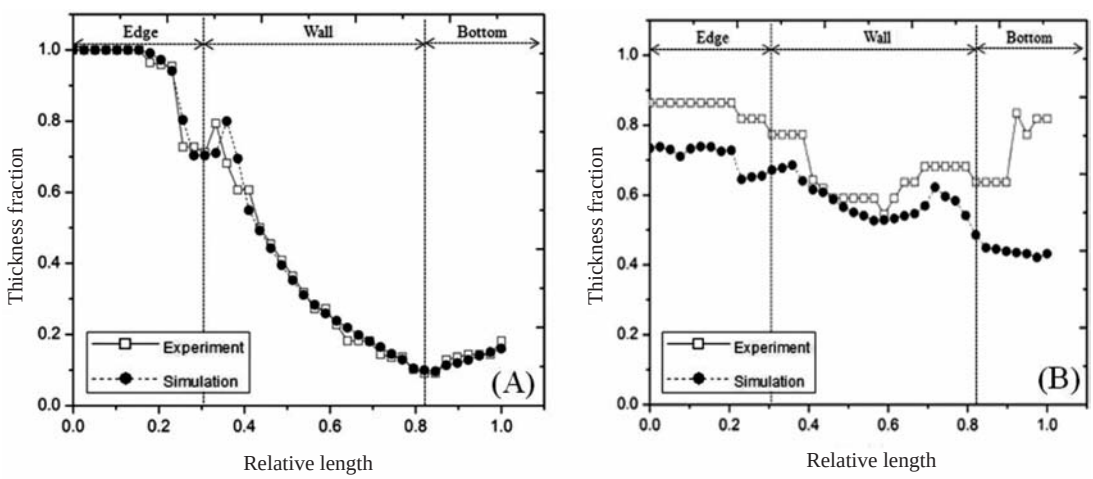

Figure 6 Comparison of predicted and experimental results using sheet and mold temperatures of 150 and 30 ^{o}C, respectively: (A) Cavity-formed part; (B) Plug-formed part.

process with no need for preliminary mold production and machine set-up, thus avoiding the time-consuming and burdensome trial-and-error process.

ACKNOWLEDGMENTS

The authors would like to express their thanks to the Wing Fung Packaging Co., Ltd., Thailand for the thermoformed mold and the cost-free supply of materials, the Industrial Technology Assistance Program (iTAP), National Science and Technology Development Agency, Thailand and the TRF-Master Research Grants for providing the financial support throughout this work (Contract grant number: MRG545E074).

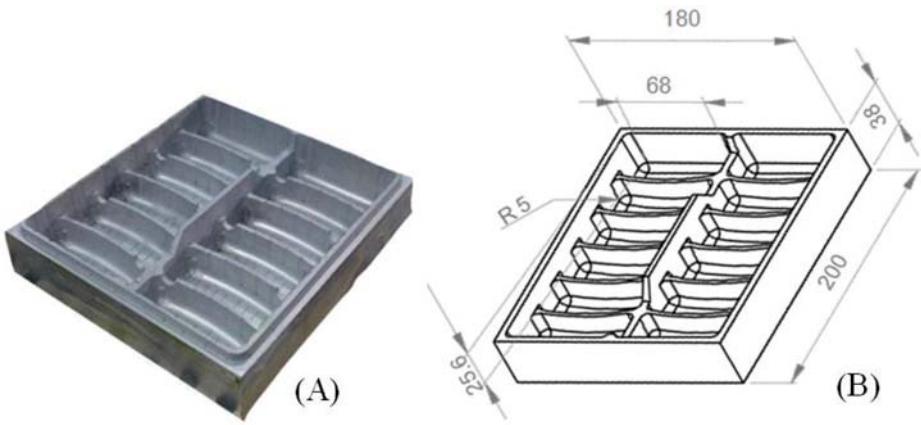

Figure 7 Complex geometry case study using a food tray: (A) Thermoformed mold; (B) Model used in the study. (All figures are distances in millimeters, R = radius.)

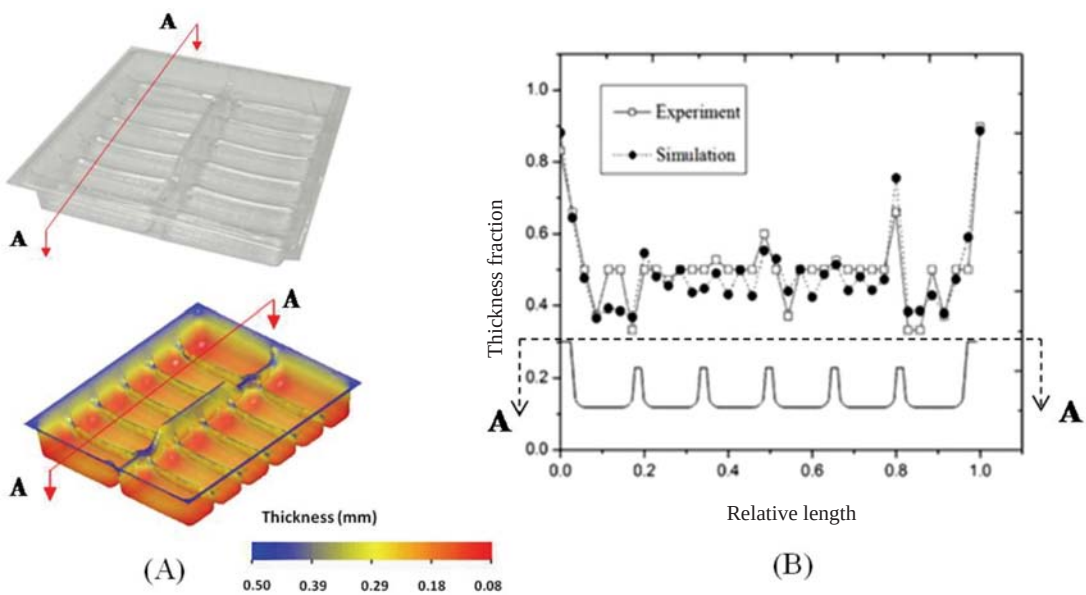

Figure 8 Comparison between predicted and measured results of wall-thickness distribution for food tray.

LITERATURE CITED

Aleksey, D.D. 1995. A constitutive model in finite viscoelasticity. **Rheol. Acta.** 34(6): 562–577.

Aroujalian, A., M.O. Ngadi and J.-P. Emond. 1997. Wall thickness distribution in plug-assist vacuum formed strawberry containers**. Polym. Eng. Sci.** 37(1): 178–182.

Bernstein, B., E.A. Kearsley and L.J. Zapas. 1963. A study of stress relaxation with finite strain. **Trans. Soc. Rheol.** 7(1): 391–410.

Dong, Y. and R.J. Lin. 2006. Finite element simulation of thermoforming acrylic sheets using dynamic explicit method. **J. Polym. Polym. Comp.** 14: 307–328.

Kaye, A. 1962. **Non-Newtonian Flow in Incompressible Fluids: Part 1 and 2 and 3.** College of Aeronautics Note 134, (now called Cranfield University). Cranfield, UK. 20 pp.

Koziey, B. 1997. New results in finite element analysis of thermoforming. **SPE ANTEC Tech. Papers** 714–719.

Lai, M.O. and D.L. Holt. 1975. Thickness variation in the thermoforming of poly(methyl methacrylate) and high-impact polystyrene sheets **J. Appl. Polym. Sci.** 19(7): 1805–1814.

Poller, S. and W. Michaeli. 1992. Film temperature. Determine the wall thickness of thermoformed parts. **SPE ANTEC Tech. Papers** 38: 104–108.

Rosenzweig, N., M. Narkis and Z. Tadmor. 1979. Wall thickness distribution in thermoforming. **Polym. Eng. Sci.** 19(13): 946–951.

Throne, J.L. 1986. **Thermoforming.** Hanser. New York, NY, USA. 862 pp.